이학석사 학위논문

Pathological characteristics of white matter in animal models for preclinical Alzheimer's disease

초기 알츠하이머병 동물모델에서

백질 내 병리학적 특징

2022 년 8 월

서울대학교 융합과학기술대학원

분자의학 및 바이오제약학과

신 진 섭

Pathological characteristics of white matter in animal models for preclinical Alzheimer's disease

지도 교수 이 동 수

이 논문을 이학석사 학위논문으로 제출함

2022 년 8 월

서울대학교 대학원

분자의학 및 바이오제약학과

신 진 섭

신진섭의 이학석사 학위논문을 인준함

2022 년 8 월

위 원 장 신 영 기 (인)

부위원장 이 동 수 (인)

위 원 최 유 리 (인)

Abstract

Jin Seop Shin

WCU, Department of Molecular Medicine and Biopharmaceutical Science,
The Graduate School of Convergence Science and Technology,
Seoul National University

Neuroinflammation, along with pathological amyloid and tau accumulation, is a major pathological hallmark of Alzheimer's disease (AD). Neuroinflammation is induced by Aβ deposition and promotes tau propagation in AD. Therefore, in preclinical AD, which is the stage of pathological changes before the diagnosis of cognitive impairment, understanding the pathologic changes is important for pathogenesis, diagnosis, and prevention, and it is necessary to understand the changes as a mediator in AD progression. To confirm pathological changes in preclinical AD, the expression of proteins related to reactive microglia and astrocytes was measured in 5XFAD with beginning Aβ formation. To observe the pathology in preclinical AD, Immunohistochemistry was performed in the 3- and 7-month-old 5XFAD animal model. As a result, glial cell reactivity and degraded myelin proteins were increased in white matter (WM) of 3-month-old 5XFAD, and lysosomal enzymes and lipid droplet were also observed. These results show that microglia and astrocytes failed to degrade myelin fragments after phagocytosis in preclinical AD. Taken together, the major pathological changes in preclinical AD occur in WM, and pathological

changes appearing in the early stages of AD are expected to provide information for early diagnosis, and development of preventive treatment.

Keywords: Alzheimer′s disease, white matter, lipotoxicity, reactive astrocyte, reactive microglia

Student number: 2020-25948

Contents

Introduction

Alzheimer's disease (AD) is a progressive neurodegenerative disease that accounts for approximately 60-80% of dementia cases. AD patients have difficulties with memory, language, problem-solving and other thinking skills. [1] In postmortem brain tissue of AD patients, pathological features are extracellular Aß accumulation, intracellular tau accumulation, and neuroinflammation. [1,2] Based on pathologic processes, the diagnosis of AD using biomarkers is grouped into ATN (amyloid, tau, and neurodegeneration) classification system published by the National Institute on Aging and Alzheimer's Association Research Framework. [3] AD-related pathological changes are expected to occur due to dysfunction of glial cell-associated immunity, lipid metabolism and endocytosis. [2]

Aß is a cleavage product of amyloid precursor protein by β-secretase and γ-secretase and initiates amyloid plaques formation pathway through oligomerization and fibrillization.[4] This amyloid deposition begins in the basal part of the frontal, temporal, and occipital lobes. [5] As amyloid accumulation progresses, it is observed in the limbic and allocortical structures, and follows by in subcortical structures including basal ganglia, selected nuclei in diencephalon and brainstem, and the cerebellar cortex. [6] Aß oligomer can promote the Aß aggregation, by fibril-forming pathway. Extracellular Aß oligomers can bind neuronal membrane receptors, and disrupts their signaling pathway, so that change the neuronal membrane permeability and integrity.

This effect can damage the cell membrane, inducing calcium influx in neuron, mitochondrial ROS production and promote tau pathologies. [7] Also Aß plaque and diffuse form of Aß can damage synapses and neurites by damaging glucose and ion transporters. [8]

Increased pathological tau in AD patients with Aß correlates with cognitive impairment. [9,10] Tau protein maintains the cytoskeletal structure of neuron through phosphorylation and dephosphorylation. In AD, excessive hyperphosphorylated tau increases in the intracellular space and forms neurofibrillary tangles (NFTs). [11] And pathological tau, like prion proteins, is propagated from neurons to the next neurons by exosomes, synaptic releases, and tunneling nanotubes. [12,13] Pathological tau in neuron directly interacts with DNA and interferes the transcription factor attachment, disrupts mitochondrial function by destabilize the microtubule, inhibiting Nicotinamide Adenine Dinucleotide Hydrogen (NADH) reduction thereby increasing the reactive oxygen species (ROS). [14-16] Also, pathologic tau induces normal tau detachment from microtubule and influences membrane permeability. [17] As a result, calcium homeostasis disruption, synapse loss, and cell death occurred. [18,19]

Furthermore, neuroinflammation is reported to play an important role in AD pathology as a mediator of tau protein propagation. [20] Microglia and astrocytes are involved in neuroinflammation, and reactive cells are observed near the Aß and tau deposits. Single-cell transcriptome studies in the AD mouse model show that homeostatic microglia transition to disease-associated microglia (DAM) with disease

progression. [21,22] In AD, DAM cannot completely degrade cellular debris and abnormal proteins, and secretes pro-inflammatory cytokines and chemokines to induce chronic neuroinflammation. [23] As AD progression, homeostatic microglia transits to DAM, with gene transcription changes, translational changes such as nuclear factor kappa light chain enhancer of activated B cells (NF-κB) activation and morphological changes and shows autophagy activity when Aß and tau exposure. However, in chronic neuroinflammation condition by Aß or tau, phagocytosis at the synapse is occurred by DAM and reactive astrocyte. Also, pro-inflammatory cytokines including tumor necrosis factor-alpha (TNF-α), interleukin-6 (IL-6) are released in microglia. As a result, DAM contributes to synaptic toxicity and spine loss. [24,25]

The most abundant glial cells of the central nervous system (CNS), astrocyte also performs play an important and has wide range of functions, including formation of blood-brain barrier (BBB) and regulating blood flow, sensing neuronal activity, transporting debris, and sensing the microenvironment. [26] Under chronic inflammation environment, reactive astrocyte alters morphology and cytokine release pattern. This cascade includes antigen presenting pathway, complement cascade. In particular, microglia influence astrocytes by cytokine/chemokine receptors directly. That receptor senses pro-inflammatory cytokine, including interferon-gamma (INF-γ), TNF-α, IL-6. This results NF-κB cascade in astrocytes, triggering excessive nitric oxide (NO) expression. [27] Also, astrocyte is impaired their ability of glutamate uptake by inflammation, and eventually induces positive feedback of neuroinflammation. [28-

30

In particular, the formation and removal of myelin is maintained through cholesterol recycling, and clearance of myelin fragments by phagocytosis of microglia and astrocytes is an essential step in the process of demyelination and remyelination balance. [31] An increase in myelin debris of white matter (WM) is observed with aging. [32] The loss of clearance function in glial cells increases glial cell reactivity and proinflammatory cytokine release. [33] And degraded myelin basic protein (dMBP) induces plaque formation by promoting the binding of Aβ fragments. [34,35] As disease progresses, the AD patient tends to increase the number of myelin fragments compared to the healthy control, and this change results in WM damage.[27]

WM damage is associated with aging. Lipid debris and droplets increases with aging, and insoluble lysosomal inclusion in microglia and lipid contents in cell increase. [36] Lipid droplets store fatty acid, and protect cells from lipotoxicity, mitochondrial damage and dysfunction. [37] However, microglia which phagocytosis excessive lipid debris reduces phagocytosis and lysosomal activity and induces transition to reactive microglia. And these reactive microglia induce chronic inflammation. [38] In addition, the increase lipid-containing cells in brain suppresses neurogenesis and affects glial phagocytosis by elevating pro-inflammatory cytokine. Lipid-containing cells impair antioxidant enzyme and autophagy pathway, which affects neuronal survival and synaptic plasticity. [41] Therefore, lipid debris derived from WM damage may influence chronic inflammation and AD progression.

Additionally, increased WM hyperintensities (WMH) on T2-weighted magnetic resonance imaging (T2-weighted MRI) scans, reflecting small vessel cerebrovascular disease (CVD), are commonly observed in AD patients. [42] WM damage, including impaired WM connectivity, is observed in patients with early-stage AD. [43] WMH is associated with cortical atrophy by aging, cognitive impairment, and transition to AD. [44-46]

Our research team analyzed the spatial transcriptome in 3- and 7-month-old 5XFAD models and found that the glial reactivity in WM was increased at the stage of initiation of amyloid deposition. At 3-month-old, 5XFAD transgenic (TG) model increased cathepsin S (CTSS), myelin associated glycoprotein at WM. [53] At 7- month-old, 5XFAD TG model increased apolipoprotein E (ApoE), complement C4b, transmembrane immune signaling adaptor (TYROBP) and triggering receptor expressed on myeloid cells (Trem2) in WM, and this upregulation was similar to GM changes. This means that changes of 3-month-old TG in WM activated neuronal ensheathment and gliosis. Also, 7-month-old TG increased reactive glial marker. These results provided clues for the WM changes in early-stage AD at RNA level and suggested the direction of the changes in preclinical AD. However, it is necessary validation at the protein level for changes in brain region-based transcriptome.

Therefore, these results help to understand WM damage and glial cell activity in early-stage AD animal models and provide information to understand the meaning of

WMH on MRI and expected to be utilized not only for mechanism research in early-stage AD, but also for diagnosis and early treatment research.

Materials and Methods

Subjects and experimental design

Male Tg6799 were maintained on a mixed C57BL/6 x SJL background and had three APP K670N/M671L + I716V + V717I mutation, two PS1 M146L + L286V mutation. 3-month-old 5XFAD, when amyloid deposition begins without changes in cognitive function, was used as a preclinical AD model. [54]

Immunohistochemistry (IHC)

1 month after BCAS surgery, mice were anesthetized with 2.5 % isoflurane delivered in 1L/min oxygen flow. And perfused with 30 mL of Saline and then fixed with 4% paraformaldehyde (PFA) and then embedded in paraffin. 4 μm thick coronal slices were used for IHC. All the slices were deparaffinated with Xylene and xylene was removed by sequential concentration of ethanol. After dehydration of Ethanol, rehydration was performed by dH2O and Tris-Buffered Saline (TBS). Then, for antigen retrieval, boil the tissue at 85 °C, 0.01M, pH 6.0 of citric acid for 10 minutes to increase the permeability of tissue using 0.5% TritonX-100 in TBS. Non-specific antigens were blocked by 5% bovine serum albumin (BSA) in TBS for 1 hour at room temperature and tissues were incubated with primary antibody, all the primary antibody was diluted in 5% BSA in TBS, overnight in the cold room. the dilution rate was as follows; S100ß [1:100; abcam, 52642], glial fibrillary acidic protein (GFAP) [1:200; cell signaling, #3670], cystatin F (CST7) [1:100; invitrogen, PA5-103772],

ionized calcium-binding adapter molecule 1 (Iba1) [1:200; abcam, ab153696], Aß [1:200; cell signaling, #8243], CTSS [1:100; invitrogen, PA5-103772], cathepsin E (CTSE) [1:100; Invitrogen, PA3-16821], dMBP [1:1,000; sigma-aldrich, AB5864], lysosomal-associated membrane protein 1 (LAMP1) [1:50; abcam, ab208943]. Tissues were fully washed with TBS and incubated with secondary antibody. all the secondary antibody was diluted in TBS, 1 hour at room temperature. The dilution rate was as follows; Alexa Flour 488 Goat anti-mouse immunoglobulin G (IgG) [1:200; invitrogen, #A11001], Alexa Flour 555 Donkey anti-rabbit IgG [1:200; invitrogen, #A31572], Goat anti-rabbit IgG [1:200; invitrogen, #A32733]. After secondary antibody staining, all the tissues were fully washed with TBS and mounted, and cover slipped. Images were captured by LEICA confocal microscopy SP8, and Metamorph image analysis software was used for quantification.

3, 3'-diaminobenzidine (DAB) staining

DAB staining kit [abcam, ab64238] is used for DAB staining. Frozen free-floating 3-and 7-month-old 5XFAD samples in glycerol were washed with phosphate-buffered saline (PBS) and treated hydrogen peroxide block for 10 minutes at room temperature and for antigen retrieval, boil the tissue at 85 °C, 0.01M, pH 6.0 of citric acid for 10 minutes to increase the permeability of tissue using 0.2% TritonX-100 in PBS. After antigen retrieval, apply protein block solution and incubate for 10 minutes at room temperature. After protein block solution treatment, tissues were incubated with primary antibody, all the primary antibody was diluted in 2% bovine serum albumin (BSA) in PBS, overnight in the cold room. After overnight, tissues were fully

washed with PBS and incubated with Biotinylated Goat anti-Polyvalent for 10 minutes at room temperature. And after apply streptavidin peroxidase 10 minute at room temperature, DAB solution is treated and incubate at room temperature. After washing, hematoxylin staining was performed 1 minutes at room temperature and washed. After hematoxylin staining, all the tissues were fully washed with PBS and mounted, and cover slipped.

Statistical analysis

For visualization and summary of the confocal image and behavioral test, Prism Graphpad was used and presented as mean ± standard deviation[55], unpaired t-test by a group. Indicated significant difference was presented as $p < 0.05$ (*), $p < 0.005$ (**).

Results

Changes in reactivity of glial cells in the brain of AD model for preclinical AD.

Aß deposition begins without cognitive impairment in the 3-month-old 5XFAD AD model similar to preclinical AD, and the 7-month-old AD model is accompanied by cognitive impairment. In the 3- and 7-month-old AD models, the expression of S100ß and CST7 was confirmed by brain region (Fig. 1a). S100ß, one of the markers of reactive astrocytes, functions as calcium flux, gliosis, and neurite extension, and CST7, whose expression is increased in reactive microglia, is a cysteine peptidase inhibitor and responds to neurotoxicity.

S100ß and CST7 protein expression was increased in WM both I.CC and E.CC of the 3-month-old TG model. However, the expression of these proteins was slightly increased, and no morphological changes were observed in GM (Fig. 1b, c). The expression of S100ß and CST7 was significantly increased in WM and GM of the 7-month-old TG model compared to those of 3-month-old TG model. In particular, there were significant changes in both expression level and morphology in the I.CC and E.CC (Fig. 1b). These changes showed that reactive glial cells were increased in the WM of preclinical AD model and were observed in WM and GM by AD progression. In order to observe pathological changes in the preclinical AD model, the CC and CA1 regions were selected as representative regions of WM and GM. The reason for selecting two regions is that 100ß and CST7 were significantly changed in CC, and CA1 is the brain region that first affected by AD, and the number of synapses

is halved in MCI, making it the most vulnerable region as AD progression.[56]

Pathological changes in the WM of the preclinical AD model.

As a result of observing amyloid pathology in CC and CA1 of AD model, Aß aggregates in CC and cytoplasmic Aß expression in CA1 were observed in 3-month-old AD model. In contrast, extracellular Aß accumulation was observed in CC and CA1 of the 7-month-old AD model (Fig. 2). In the 7-month-old TG model, I observed that the expression of S100ß and GFAP, reactive astrocyte markers, and CST7 and Iba1, reactive microglia markers, in line with increased Aß deposition. Reactive glial cell-associated proteins were increased in CC of 3-month-old TG, and their morphologic change was also observed. On the other hand, although cytoplasmic Aß accumulation was observed, reactive glial cell was not significantly increased at CA1 region of 3-month-old TG. (Fig. 2, 3). These changes demonstrated that the glial cells in WM were functionally as well as structurally altered in the preclinical AD model.

To investigate the reactivity of glial cell, I stained the lysosomal enzyme, CTSS and CTSE. Lysosomal peptidase for degrading pathogens such as Aß also increased with AD progression. CTSS, which associated with major histocompatibility complex 2 (MHC2) -related antigens representation, increased with increasing reactive glial cells at CC of 3-month-old TG. And CTSE, which degrades bulk proteins in the lysosome, CTSE expression was also significantly increased in CC of 3-month-old TG compared to age-matched WT (Fig. 4). However, CTSS and CTSE expression

did not change in CA1 of 3-month-old TG model (Fig. 4b). On the other hand, CTSS and CTSE expression was significantly increased in CC and CA1 of 7-month-old TG compared to age-matched WT (Fig. 4). Therefore, the expression of lysosomal enzymes increased, similar to the pattern of increased reactivity of glial cells.

To demonstrate the cause of the increase in reactive glial cells and lysosomal enzymes, myelin proteins were observed. MAG, a myelin protein that anchors axons and myelin sheath, was increased in CC of both 3- and 7-month-old TG models compared to age-matched WT as spatial transcriptomics data demonstrated. Also, I observed the disorganized MAG was increased in the CC and subcortical region. And MAG expression in GM was only increased at 7-month-old TG model. Also, I stained dMBP. A degraded form of MBP indicate myelin damage because MBP constitutes myelin sheath. dMBP was significantly increased in both CA1 and CC of 7-month-old TG model, but dMBP was not significantly increased in GM at 3-month-old TG. In addition, dMBP was significantly increased at CC and subcortical region of CC. As a result of observing myelin damage, myelin damage started to increase in at 3-month-old TG as the expression of reactive glial cells increased. (Fig. 5).

At last, factors that affect the increase of reactive glial cells were investigated. Insoluble lipid droplets in reactive glial cells induce the chronic inflammation and induce homeostatic glial cells into reactive glial cells. [36] Insoluble lipid droplets, lipofuscin was increased at CC of both 3- and 7-month-old TG compared to age-matched WT. In CC, lipofuscin was also found in subcortical regions. And lipofuscin

was increased in CA1 of 7-month-old TG. And, I stained with cell markers to determine which cells had increased lipofuscin. In 7-month-old TG, the tissue was stained with NeuN, a neural marker, GFAP, a reactive astrocyte, or Iba1, a microglia marker, and overlap with lipofuscin was confirmed. The formation of lipofuscin was usually observed in neuron with aging and was increased in neuron of 7-month-old TG. Specifically, an increase in lipofuscin was also observed in reactive glial cells t. (Fig. 6)

In addition, LAMP1, a lysosomal membrane protein, was stained to confirm the state of neurons when Aβ accumulates in the cytoplasm and WM damage appears. Staining of LAMP1 in axons around amyloid indicates dystrophic neurites. The accumulation of LAMP1 was significantly increased in CC at 3-month-old and 7-month-old TG. However, LAMP1 expression was not significantly increased at CA1 of the 3-month-old TG. (Fig. 7) Therefore, pathological changes in preclinical AD were observed with myelin damage in the WM and an increase in lysosome-related degrading enzymes. It was characterized by increased glial cell reactivity and axonal damage.

Discussion

In AD progression, Braak stage was suggested based on the results of observation of pathological changes, and it is divided into mild cognitive impairment, mild-, moderate-, and severe-AD based on symptoms. With development of biomarkers, changes in Aβ occur 20 years before the onset of symptoms. Therefore, individuals with no symptoms and changes in Aβ are called preclinical AD in AD continuum. Early diagnosis and prevention of AD, before irreversible brain damage or cognitive impairment, is focused on attention as a new treatment strategy. Consequently, understanding the brain cell changes that occur in preclinical AD provides basic information for earlier diagnosis and prevention.

In this study, 5XFAD was used as an animal model to understand preclinical AD. 5XFAD mice have Swedish (K670N/M671L), Florida(I716V), and London (V717I) mutation in APP and M146L and L286 mutation in presenilin-1 (PSEN1). Intracellular Aß42 is detected at about 6 weeks, and reactive astrocytes and microglia are detected about 8-week-old mouse. [57] Also, hippocampal atrophy and global neuron death can be seen about 6-month-old, accompanied by cognitive impairment. [54,58] Since amyloid deposit begins first, it is a suitable model for early diagnosis. Therefore, a model in which amyloid deposition is the main change is suitable for preclinical AD research and early diagnosis.

Pathological changes in AD were considered GM disease in the past. However,

neuroimaging studies have revealed that demyelination and WM damage precede to GM damage and cognitive impairment. [59-61] Myelin sheath tends to damage and thinned by aging and AD progression. On the other hand, thin myelin sheath increases unmyelinated fiber and demyelination, and the exposed unmyelinated fibers are vulnerable to harmful substances such as Aß and oxidative stress, resulting neurotoxicity and neuronecrosis. [62]

To observe pathological changes in animal models reflecting preclinical AD, I observed various WM and GM regions to select representative images. I analyzed GM including dentate gyrus, CA1, CA3, retrosplenial cortex, somatosensory cortex, thalamus. At 7-month-old TG, reactive glial cells were increased in all GM areas, but no significant change was observed at 3-month-old TG. (Fig. 1b, c) Among the various regions, I selected CA1 because CA1 is important for memory and selectively degenerated in early-stage AD. The CA1 region of the hippocampus is vulnerable to abnormal amyloid and tau proteins and especially pyramidal neurons within CA1 are vulnerable in AD. And synapse number of pyramidal neurons is significantly decrease as AD progression. [56,63] Also, exposed afferent dendrite of GABAergic interneuron at CA1 region cause dendritic loss and neuronal loss by Aß toxicity. [64,65] And I also analyzed WM including corpus callosum, fimbria, internal capsule, cerebral peduncle. I selected corpus callosum because significantly increased expression pattern of reactive glial cells was observed in the CC of 3-month-old TG. Also, corpus callosum connects the left and right cerebral hemispheres and is the largest WM region in the brain. And this region is known as a vulnerable area in AD patients, and lesion can be

detected early-stage AD. [66,67] It was confirmed that the reactivity of glial cells proceeded in the corpus callosum in the initial stage of amyloid deposition. (Fig. 2a) Also, increase in neuroinflammation has been reported with amyloid deposition in the early-stage AD. (Fig. 2, 3) To observe the characteristics, markers of reactive glial cells were observed. The morphological change of astrocytes was measured by GFAP staining. The expression of GFAP, a type III intermediate filament protein, is upregulated in the astrocytes of glia limitans and in reactive astrocytes. Also, GFAP is involved in cell communication and the blood brain barrier function. And GFAP expression is regulated by physiological stimuli such as physical activity, enriched environmental exposure, and glucocorticoids, and fluctuates according to the circadian rhythms in the suprachiasmatic nucleus.

Changes in GFAP expression may also reflect physiological adaptive plasticity and abnormality rather than being simply a reactive response to pathological stimuli. [55,68,69] Although the increase of GFAP expression indicates changes in astrocytes through morphological remodeling, I also observed S100ß related to cell signaling to further confirm functional changes. [53] Cytoplasmic enzyme S100ß staining does not exhibit small processes like GFAP staining but can visualize somatic and proximal processes in astrocytes. S100ß regulates calcium flux, gliosis, and neurite extension. It interacts with cytoskeletal proteins such as GFAP to regulate cytoskeletal structure and inhibits polymerization of GFAP dimers. [70] In pathologic condition, S100ß expression increases and S100ß induces neuritic plaque formation. [71] In addition, increased expression of Iba1 is a marker for ramified and reactive microglia. This molecule is involved in microglial movement and phagocytosis by crosslinking of

actin and membrane ruffling. Thus, an increase of Iba1 expression appears in the morphological change from quiescent branched microglia to activated amoeboid microglia in the disease condition. [72] CST7 is a highly expressed cysteine peptidase inhibitor in microglia in response to neurotoxicity and is one of the genes increased in DAM. It functions as a negative regulator of protease binding and peptidase activity in the extracellular region. [73] Therefore, morphological changes and CST7 expression indicate altered microglial reactivity. And it has been reported that the ferritin light chain (FTL), iron storage protein, is condensed in Aß or tau-loaded glial cells, and FTL-positive glial cells represent reactive microglia. [74] As a result of staining using these markers, reactive microglia and astrocytes appeared earlier in WM than in GM when amyloid began to accumulate.

In order to confirm the lysosomal characteristics of reactive glial cells in WM, I observed the protease of the endosomal-lysosomal system. (Fig. 4) CTSS is a cysteine protease that degrades antigenic proteins to present MHC2 molecules and plays an important role in antigen-presenting and pro-inflammatory cytokine release. [75,89] For this reason, CTSS expression is observed mainly in antigen presenting cell such as reactive glial cells. [76] And the main function of CTSE, an aspartic endopeptidase, is to degrade proteins by bulk proteolysis in lysosomes. CTSE is only detected in pathological tissues, including AD brain, not detected in young and healthy brain. [77] Microglia expressing CTSE induces neuroinflammation, plaque deposition, cognitive impairment in mouse and patients with AD. [78] Expression of these peptidases was increased in WM of 3-month-old TG and was increased lysosomal enzyme expression

level in GM of only 7-month-old TG according to the increase in the expression of reactive glial cell.

I tried to figure out the agents which affects the increased level of lysosomal enzymes and increased level of reactive glial cells. As the reactivity of glial cells increase, myelin protein damage was observed in WM. (Fig. 6) Oligodendrocytes in the CNS can generate myelin sheath and express myelin proteins, including myelin proteolipid protein (PLP), myelin basic protein (MBP), MAG and CNP 2′,3′-cyclic nucleotide 3′-phosphodiesterase (CNP). [69] Myelin surrounds the axon with a multilayered membrane of lipids. Myelin protects axons and insulates neurons, helping them conduct electrical signals. [79] MAG is located in the inner membrane of oligodendrocytes and interconnects the myelin sheath and the axon membrane. PLP and MBP are distributed within the myelin sheath and interact between the multilayered structures of myelin for compression. And the half-life of myelin membrane components varies from several weeks to several month. [33] Microglia and astrocytes play important roles in degraded myelin phagocytosis and proper myelination for degeneration and regeneration of the myelin sheath by cholesterol recycling. [80] The recent study shows that myelin damage occurs before Aß and NFT deposition in preclinical AD. Reduced myelination and MBP increase Aß42 accumulation, and demyelination are associated with AD progression. [81-83] Local demyelination was observed near Aß in the neocortex in patients with AD, suggesting that Aß-mediated demyelination induces neuronal and axonal damage. [84] In addition, accelerated remyelination in the AD mouse model improved cognition and

hippocampal atrophy. [85] In this study, I observed increases in lipofuscin concurrently with MAG and degraded MBP in 3-month-old TG (Fig. 6). These results imply that myelin sheath damage at WM and an overload of glial degradation function. As aging, myelin fragmentation increases and the burden of myelin degradation on microglia increases. Thus, microglia demonstrate the characteristics of senescence with increased lysosomal inclusions such as lipofuscin. [33] Additionally, in chronic neuroinflammatory conditions such as AD, clearance function of immune cells is reduced.[67] As a result, excessive myelin debris induced by WM damage can overburden the glial cells which phagocytosis and degrades myelin debris, so that lysosomal activity was increased. However, glial cell cannot digest all the myelin debris, so lipofuscin can be increased in glial cells. Increased lipofuscin in homeostatic glial cells induce chronic inflammation and transit homeostatic glial cells to reactive glial cells. Therefore, changes in WM occur in the early-stage AD, and these changes are manifested in increased glial cell reactivity.

Finally, I was observed axonal damage to determine the state of neurons in the presence of WM damage. LAMP1 is a pre-mature lysosomal marker, and premature lysosomes are expressed by neuronal autophagy and endocytic pathway. Pre-mature lysosomes become mature lysosomes near the cell body by retrograde transport. However, when pathologic substances such as plaques are present around the axon, blockade of pre-mature lysosomal vesicle transport occurs, resulting in LAMP1 accumulation in the vicinity of Aß. [86,87] Axonal damage was detected in 3-month-old TG following increasing WM damage and reactive glial cell. And axonal damage was

significantly increased in CA1 of 7-month-old TG compared to age-matched WT. Therefore, it was found that axonal damage occurred earlier in WM than in GM.

Understanding the characteristics of preclinical AD through spatial transcriptome analysis has limitations in identifying causes and consequences over time. In other words, the results of verifying the changes in the transcriptome of the tissue section were analyzed by synthesizing the literatures studied so far. As a result, it was observed that WM damage induces phagocytosis of glial cells, and lysosomal activity of glial cells also increases. However, glial cells cannot digest all phagocytosed myelin debris, thereby insoluble lipid droplet, lipofuscin increases in the glial cells. Increased lipofuscin in glial cells induces chronic inflammation, and dystrophic neurons are also increased in the WM. Therefore, the pathological changes in WM are characteristic changes of preclinical AD, and these changes are associated initiation of AD progression. In addition, these features of preclinical AD can be utilized as information for early diagnosis and prevention

Figures

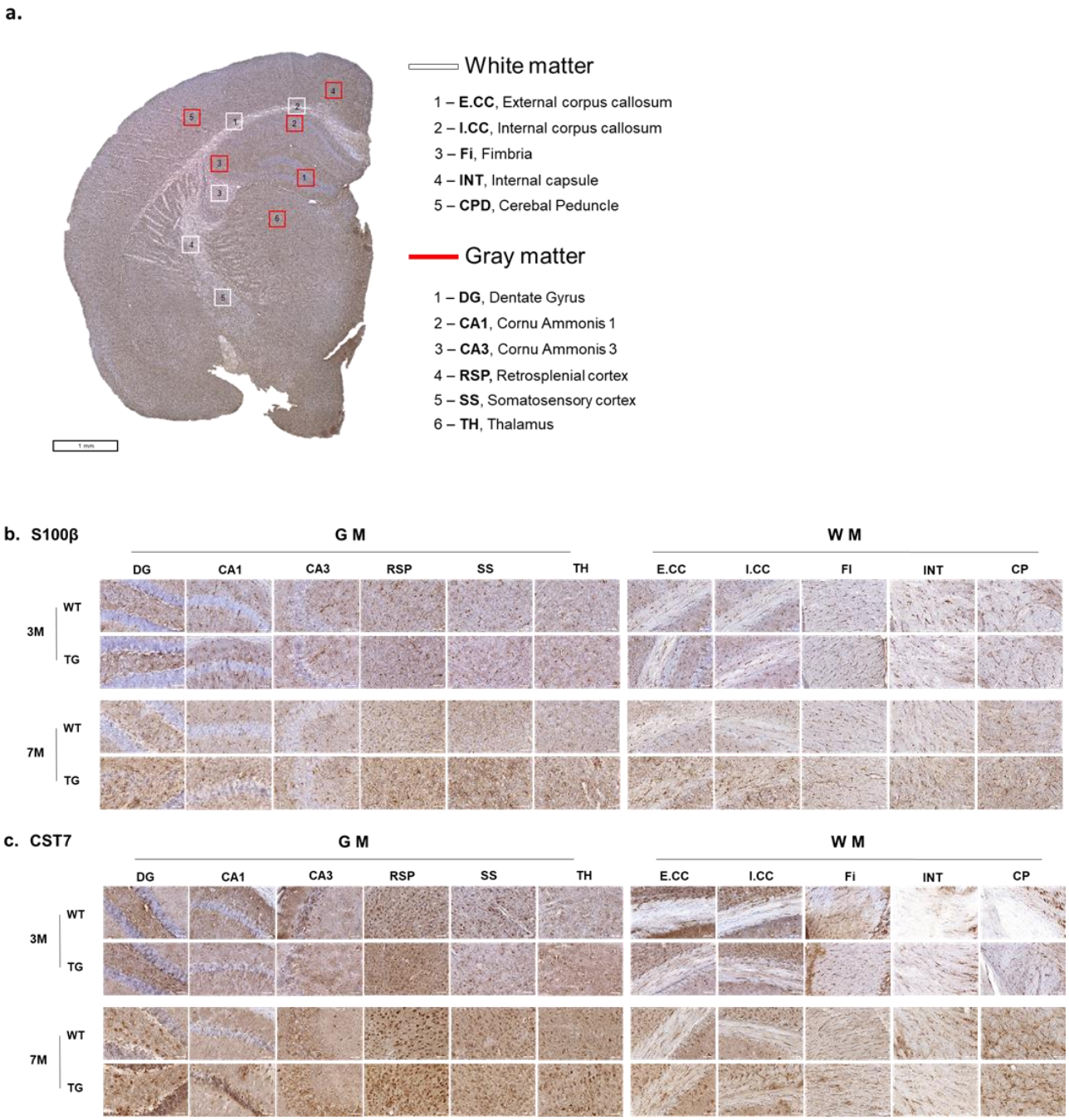
a.
White matter
1 – E.CC, External corpus callosum
2 – I.CC, Internal corpus callosum
3 – Fi, Fimbria
4 – INT, Internal capsule
5 – CPD, Cerebal Peduncle
Gray matter
1 – DG, Dentate Gyrus
2 – CA1, Cornu Ammonis 1
3 – CA3, Cornu Ammonis 3
4 – RSP, Retrosplenial cortex
5 – SS, Somatosensory cortex
6 – TH, Thalamus
1 mm
b. S100β
G M
W M
DG
CA1
CA3
RSP
SS
TH
E.CC
I.CC
FI
INT
CP
3M
7M
WT
TG
c. CST7
G M
W M
DG
CA1
CA3
RSP
SS
TH
E.CC
I.CC
Fi
INT
CP
3M
7M
WT
TG

Figure 1. Reactivity of glial cells by brain region in AD model.

Immunostaining with S100β was performed on coronal sections of the brain in 3- and 7-month-old AD models. WM (white box) and GM (red box) areas where glial cells were observed for reactive changes are indicated (a). Representative images of S100β for observing reactive astrocytes and CST7 for observing reactive microglia (b, c). The corpus callosum [88] region of WM and CA1 region of GM, where changes in reactive glial cells are observed, were selected as representative regions, respectively. scale bars represent 1 mm (a) and 50 μm (b, c), respectively.

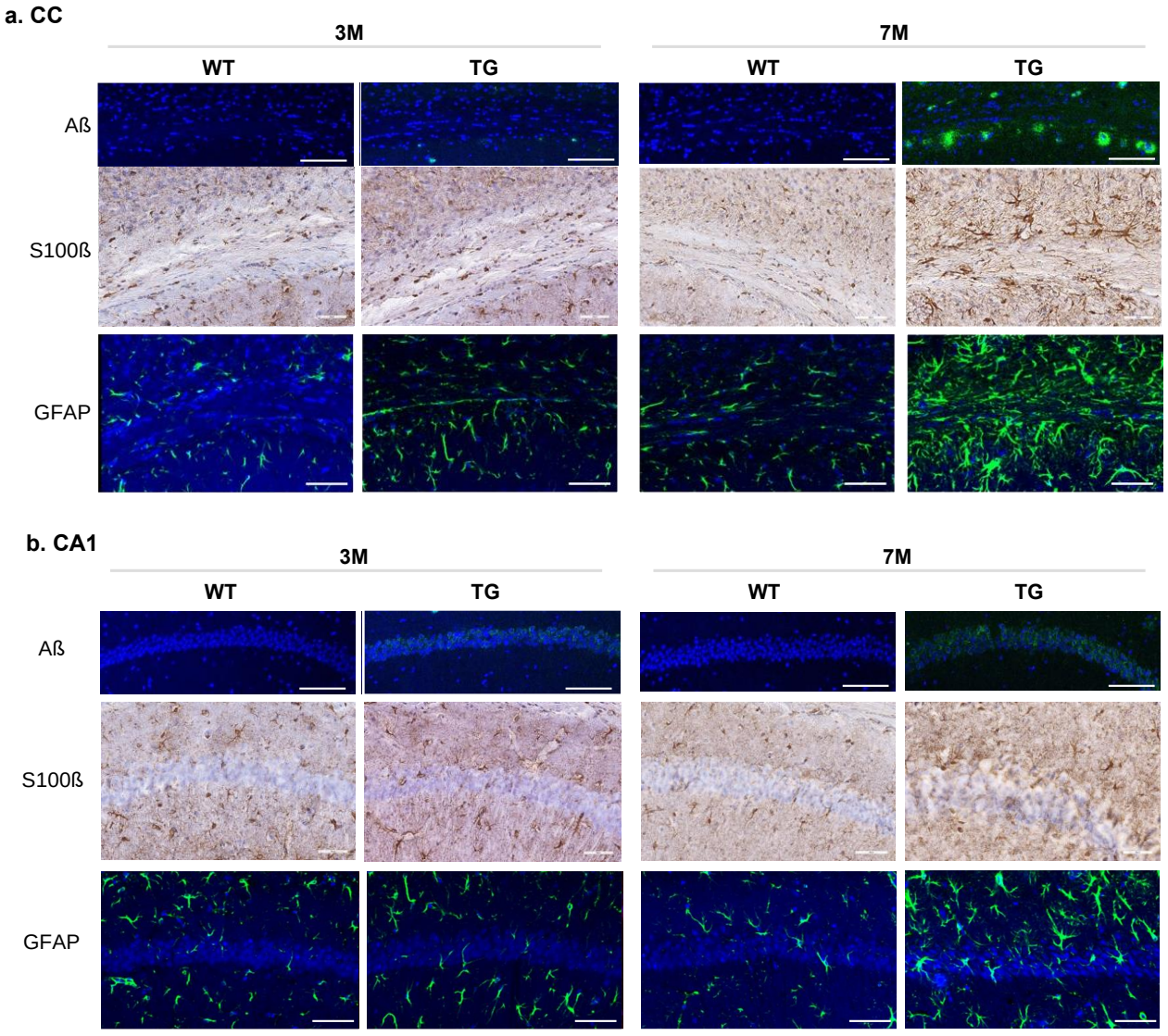
a. CC
3M
7M
WT
TG
WT
TG
Aß
S100ß
GFAP
b. CA1
3M
7M
WT
TG
WT
TG
Aß
S100ß
GFAP

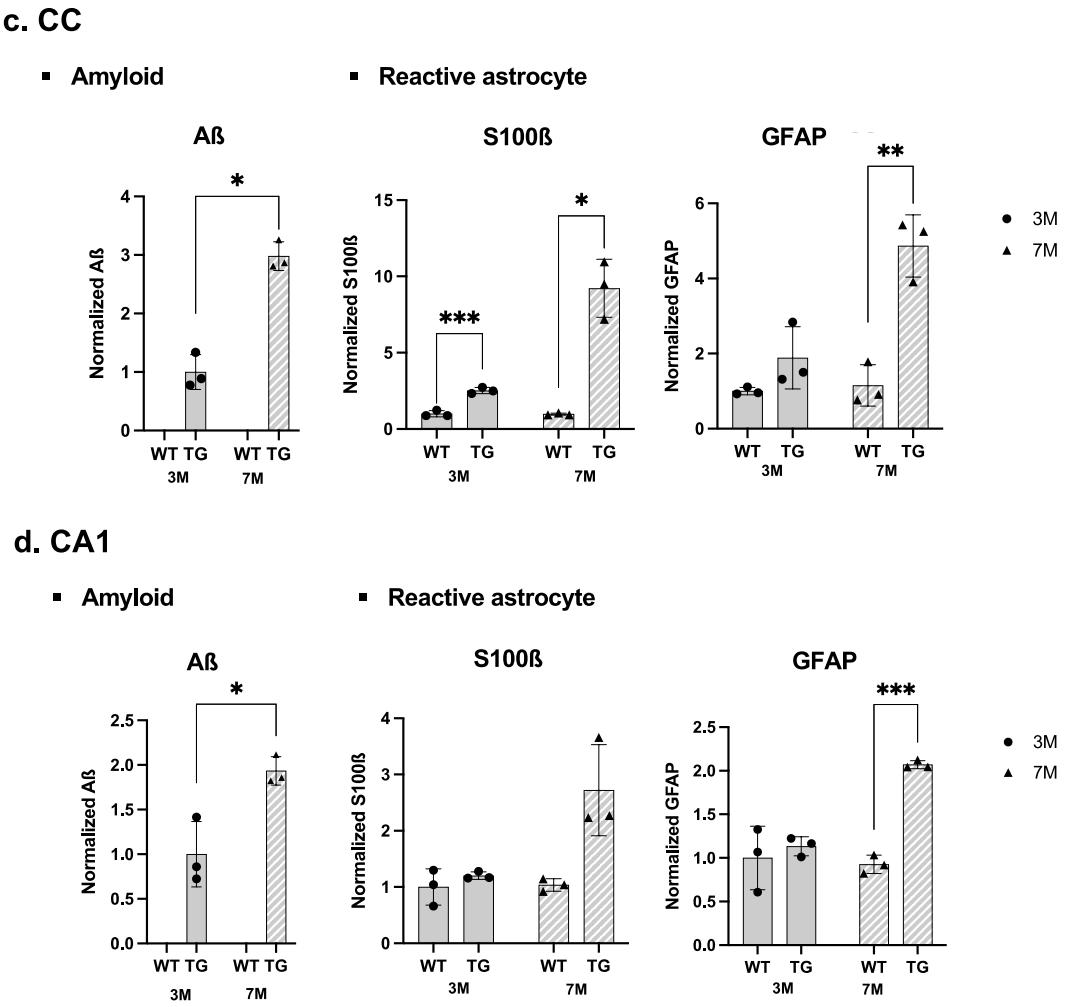

Figure 2. Aβ accumulation and reactive astrocyte in 3- and 7-month AD model.

Representative DAB and fluorescence images of Aß (green) or GFAP (green) and nucleus (blue) staining in the CC and CA1. Aβ accumulation was observed intracellularly in 3-month-old TG, whereas Aβ accumulation was increased and observed extracellularly in 7-month-old TG. Also, reactive astrocyte was increased at CC in 3-month-old TG, whereas reactive astrocyte was increased at CA1 in 7-month-old TG. Scale bars = 50 μm.

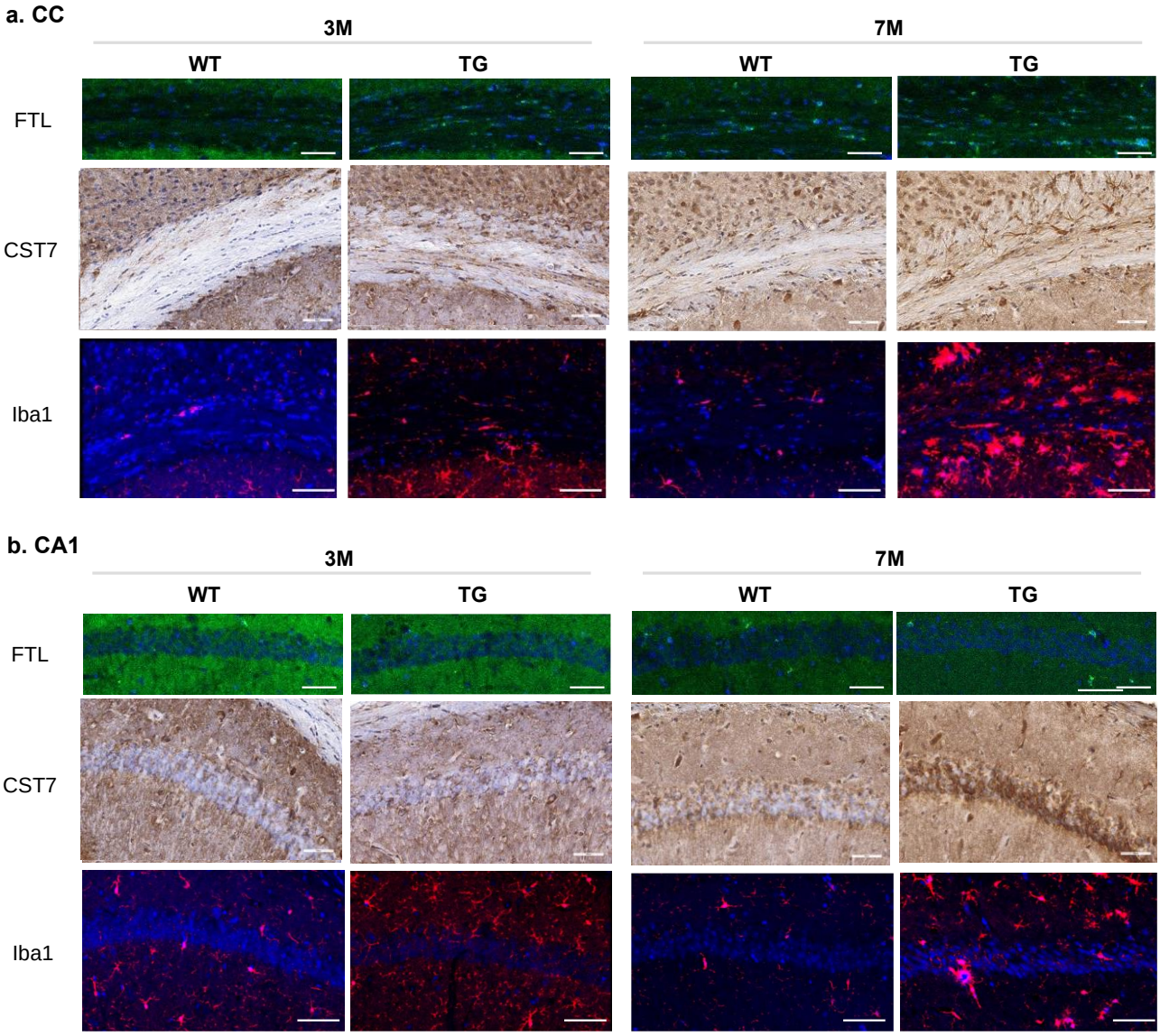
a. CC
3M
7M
WT
TG
WT
TG
FTL
CST7
Iba1
b. CA1
3M
7M
WT
TG
WT
TG
FTL
CST7
Iba1

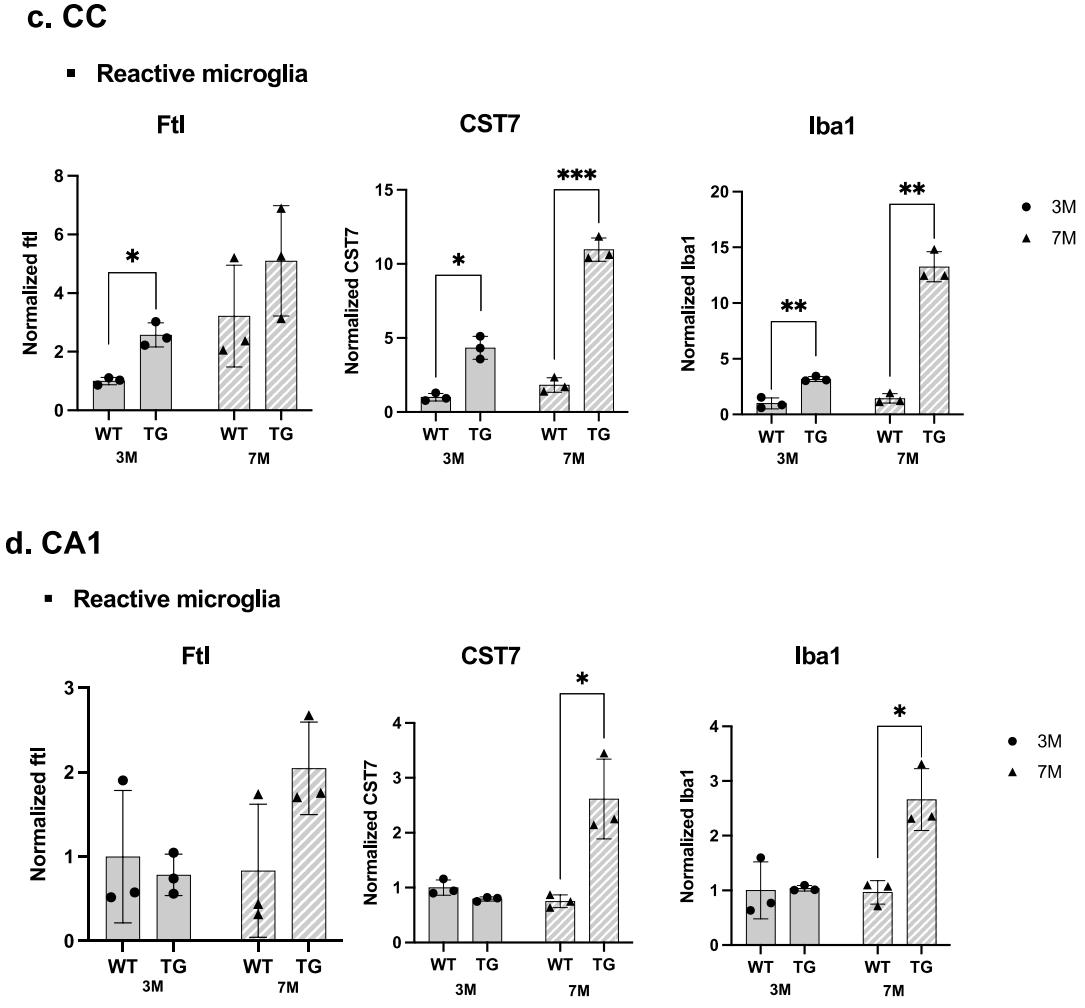

Figure 3. Reactivity of microglia in CC and CA1 of 3- and 7-month-old AD model.

Representative DAB and fluorescence images of reactive glial cells in the CC and CA1. Reactive microglia increased in 3-month-old TG and significantly increased at CC in 3-month-old TG, whereas reactive microglia at CA1 was significantly increased in 7-month-old TG. Scale bars = 50 μm

a. CC

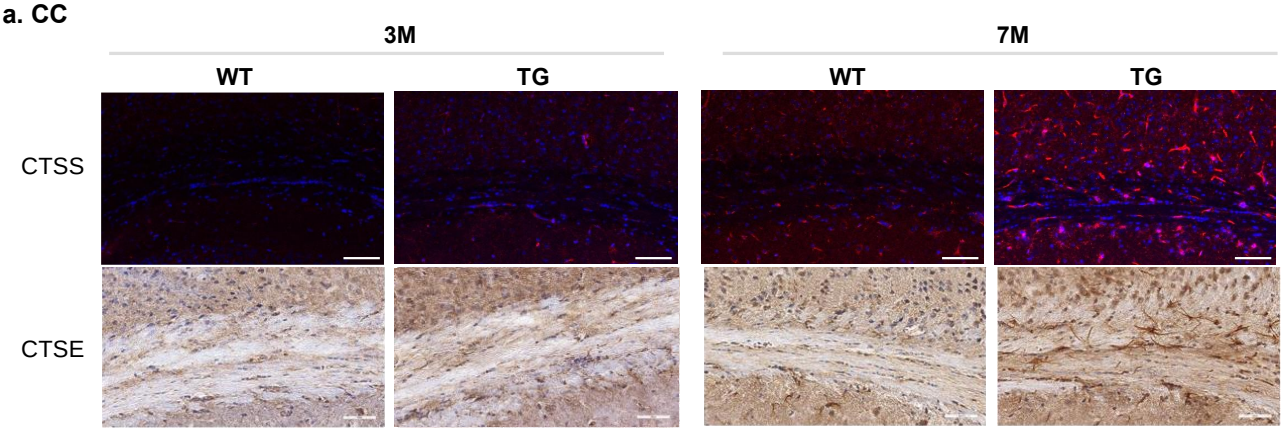

b. CA1

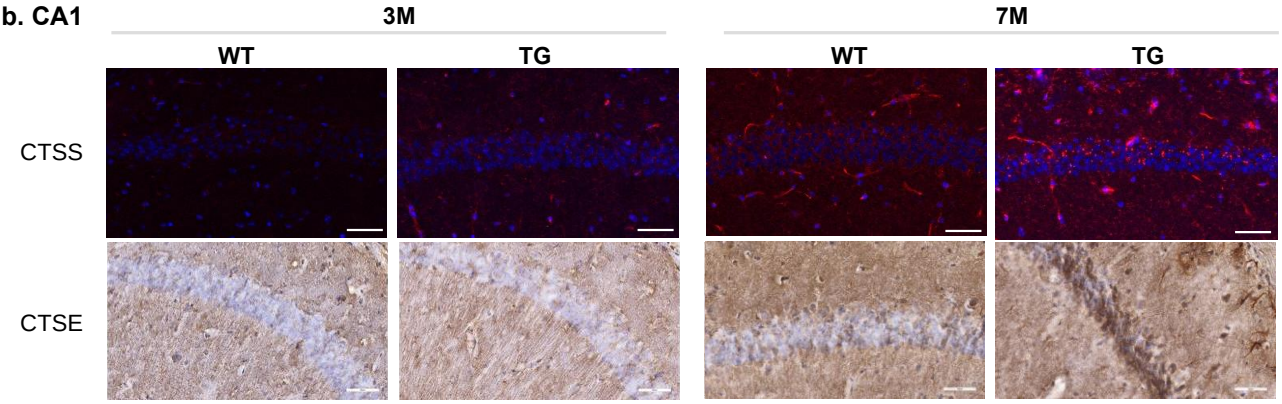

c. CC

- Lysosomal enzyme

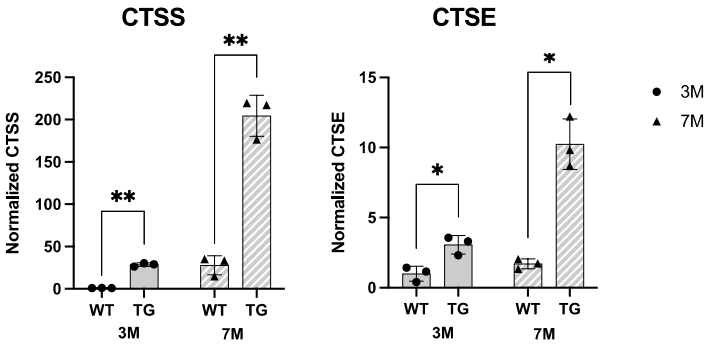

d. CA1

- **Lysosomal enzyme**

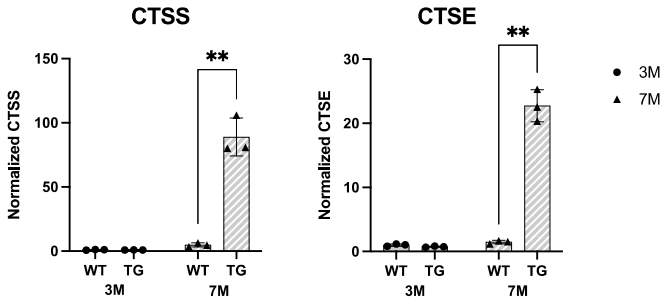

Figure 4. Accumulation of lysosomal degrading enzymes in CC and CA1 of 3- and 7-month AD model.

Representative images of CTSS and CTSE (brown), which are lysosomal proteases, in CC and CA1. Expression level of CTSS and CTSE in CC were significantly increased in 3-month TG and at 7-month-old TG, both CC and CA1 of CTSS and CTSE were increased compared to WT. Scale bars=50 μm

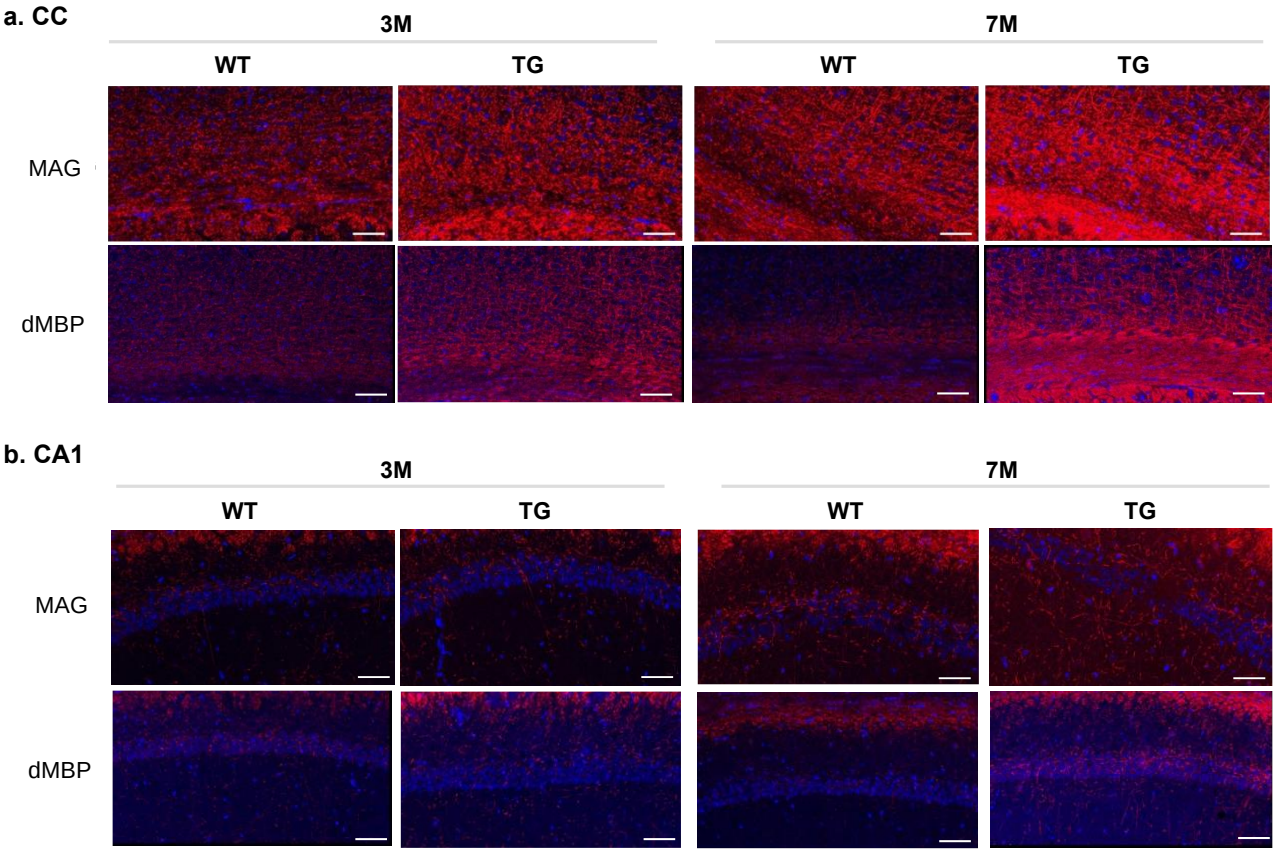

c. CC

- **White matter damage**

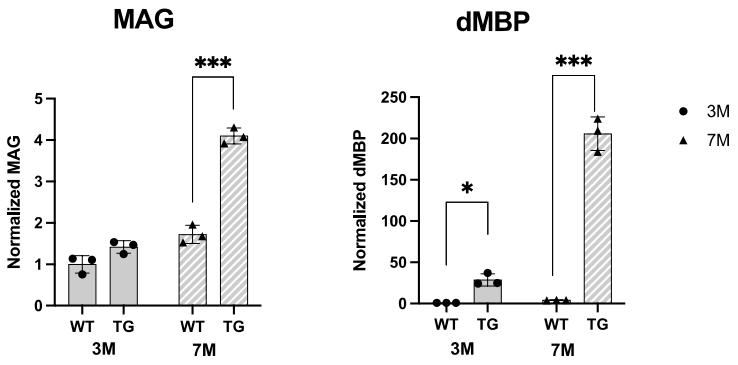

d. CA1

- **White matter damage**

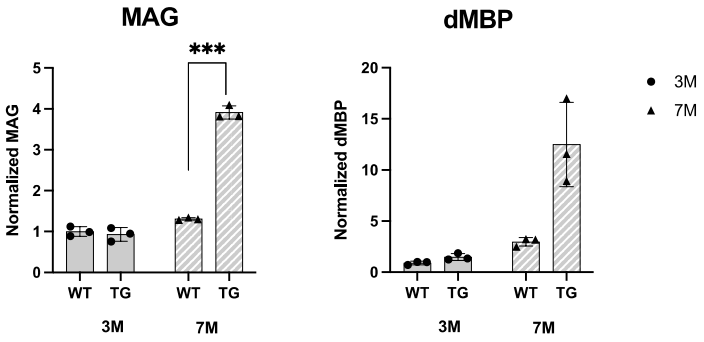

Figure 5. Changes in white matter damage in 3- and 7-month-old AD model.

Representative images of MAG and degraded MBP staining in 3- and 7-month-old TG. Increased expression and disorganization of MAG was observed at CC in 3-month-old TG, and dMBP expression was also increased at CC in 3-month-old TG. At CA1 region, MAG and dMBP expression was increased only in 7-month-old TG. Scale bars = 50 μm

a. CC

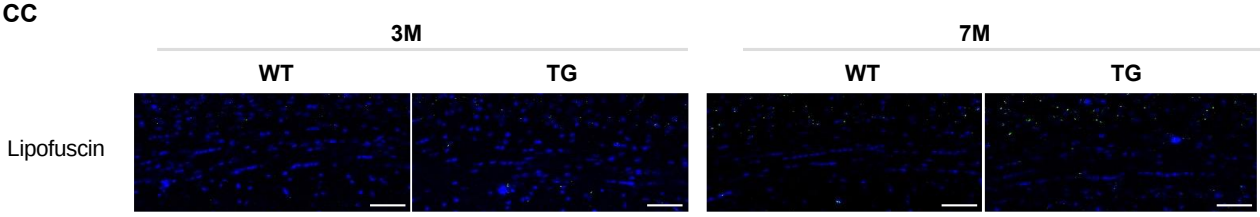

b. CA1

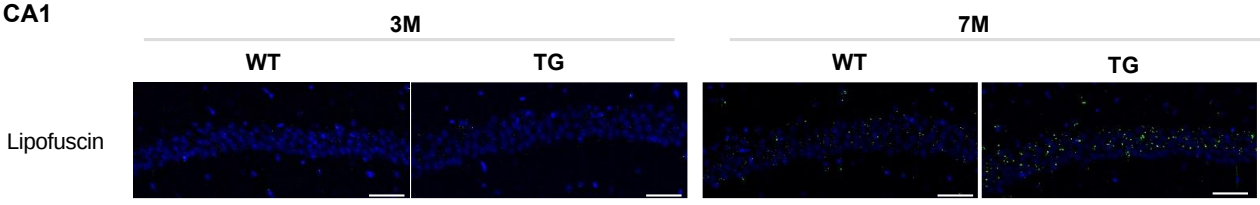

c. CC

- White matter damage

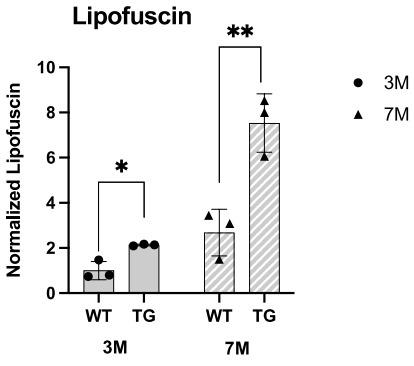

d. CA1

- White matter damage

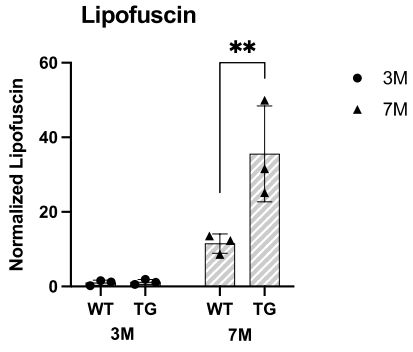

e.

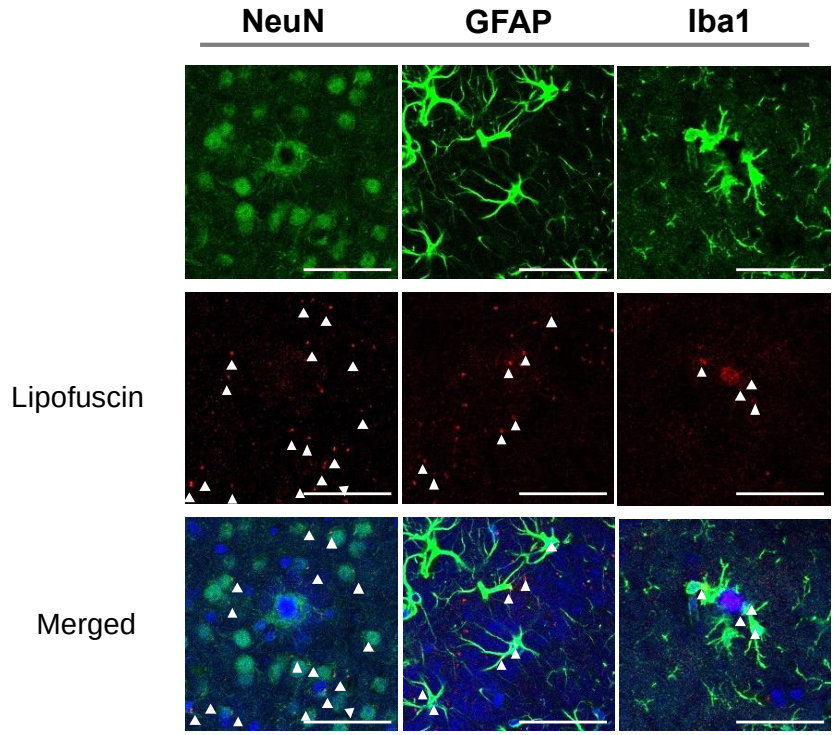

Figure 6. Lipofuscin in 3- and 7-month-old AD model.

Representative images of lipofuscin staining in 3- and 7-month-pold TG. Lipofuscin expression was increased at CC in 3-month-old TG. At CA1, lipofuscin expression was increased only in 7-month-old TG. In addition to lipofuscin was overlapped with NeuN, lipofuscin was also overlapped with GFAP, Iba1 at 7-month-old TG. (e) Scale bars = 50 μm

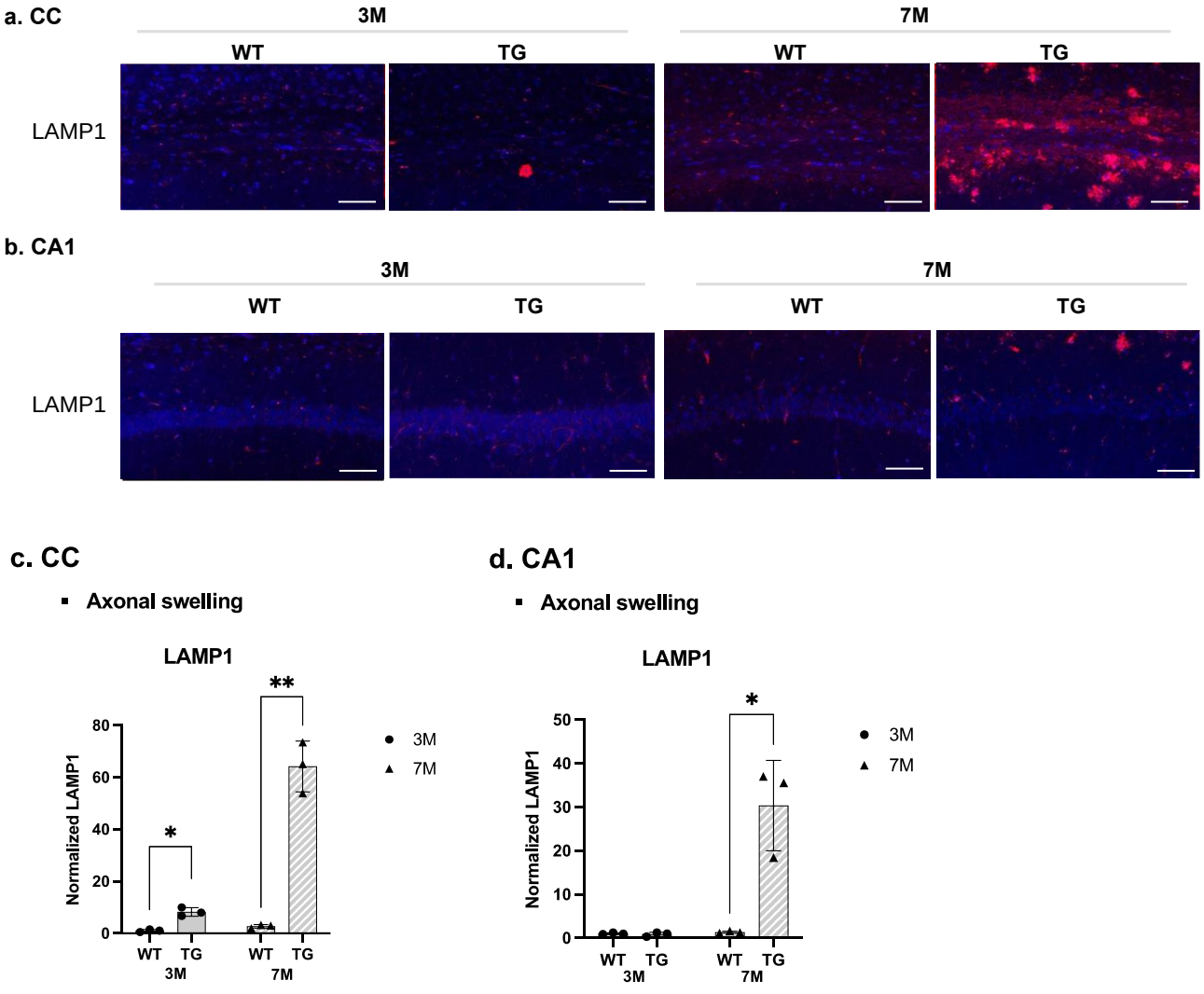

Figure 7. Changes in axonal swelling in 3- and 7-month-old AD model.

Representative images of LAMP1 in CC and CA1. LAMP1 expression was significantly increased near the CC of 3-month-old TG and LAMP1 expression was significantly increased in CC and CA1 of 7-month-old TG. Scale bars = 50 μm

초 록

신 진 섭

서울대학교 융합과학기술대학원

분자의학 및 바이오제약학과

병적 아밀로이드 및 타우 축적과 함께 신경염증은 알츠하이머병의 주요 병리학적 특징이다. 알츠하이머병에서 신경염증은 아밀로이드 침착에 의해 유도되고, 타우 전파를 촉진한다. 알츠하이머병의 초기 병리학적 변화를 이해하는 것은 발병기전 및 진단과 예방에 중요하며, 이러한 초기 변화는 알츠하이머병 진행의 매개체로서 연구가 필요하다. 따라서, 본 연구는 초기 알츠하이머병의 병리학적 변화를 확인하기 위해 반응성 미세아교세포 및 성상세포와 관련된 단백질의 발현을 아밀로이드 형성이 시작되는 알츠하이머병 동물모델(5XFAD)에서 관찰했다. 초기 알츠하이머병의 병리를 관찰하기 위해서, 3개월과 7개월 5XFAD 동물 모델에서 면역조직염색법을 수행했으며, 알츠하이머병의 위험인자 중 하나인 혈류 저하가 병리적 변화를 유발하는지 관찰하였다. 그 결과, 3개월의 5XFAD 백질에서 반응성 아교세포들과 미엘린 단편의 증가를 확인했다. 더불어 리소좀 분해 효소들의 증가와 분해되지 않은 지질 방울들의 증가가 관찰되었다. 이러한 결과는 미세아교세포와 성상세포가 초기 알츠하이머 병에서 식균작용 후 미엘린 단편을 분해하지 못한 것을

보여준다. 따라서 초기 알츠하이머병에서 백질 내 병리적 특징을 이용하여 알츠하이머병 조기진단 및 예방 치료제 개발에 활용할 수 있다.

핵심어 : 알츠하이머병, 백질, 지방 독성, 반응성 미세아교세포, 반응성 성상교세포
학 번 : 2020-25948

References

1 2021 Alzheimer's disease facts and figures. *Alzheimers Dement* **17**, 327-406, doi:10.1002/alz.12328 (2021).

2 van der Kant, R., Goldstein, L. S. B. & Ossenkoppele, R. Amyloid-β-independent regulators of tau pathology in Alzheimer disease. *Nat Rev Neurosci* **21**, 21-35, doi:10.1038/s41583-019-0240-3 (2020).

3 Jack, C. R., Jr. *et al.* NIA-AA Research Framework: Toward a biological definition of Alzheimer's disease. *Alzheimers Dement* **14**, 535-562, doi:10.1016/j.jalz.2018.02.018 (2018).

4 Srinivasan, K. *et al.* Untangling the brain's neuroinflammatory and neurodegenerative transcriptional responses. *Nature Communications* **7**, 11295, doi:10.1038/ncomms11295 (2016).

5 Palmqvist, S. *et al.* Earliest accumulation of β-amyloid occurs within the default-mode network and concurrently affects brain connectivity. *Nature Communications* **8**, 1214, doi:10.1038/s41467-017-01150-x (2017).

6 Braak, H. & Braak, E. Neuropathological stageing of Alzheimer-related changes. *Acta Neuropathol* **82**, 239-259, doi:10.1007/bf00308809 (1991).

7 Huang, Y.-r. & Liu, R.-t. The Toxicity and Polymorphism of β-Amyloid Oligomers. *International Journal of Molecular Sciences* **21**, 4477 (2020).

8 Chen, G.-f. *et al.* Amyloid beta: structure, biology and structure-based therapeutic development. *Acta Pharmacologica Sinica* **38**, 1205-1235, doi:10.1038/aps.2017.28 (2017).

9 Betthauser, T. J. *et al.* Amyloid and tau imaging biomarkers explain cognitive decline from late middle-age. *Brain* **143**, 320-335, doi:10.1093/brain/awz378 (2020).

10 La Joie, R. *et al.* Prospective longitudinal atrophy in Alzheimer's disease correlates with the intensity and topography of baseline tau-PET. *Sci Transl Med* **12**, doi:10.1126/scitranslmed.aau5732 (2020).

11 Takeda, S. Tau Propagation as a Diagnostic and Therapeutic Target for Dementia: Potentials and Unanswered Questions. *Frontiers in neuroscience* **13**, 1274-1274, doi:10.3389/fnins.2019.01274 (2019).

12 Wang, Y. *et al.* The release and trans-synaptic transmission of Tau via exosomes. *Molecular Neurodegeneration* **12**, 5, doi:10.1186/s13024-016-0143-y (2017).

13 Brunello, C. A., Merezhko, M., Uronen, R.-L. & Huttunen, H. J. Mechanisms of secretion and spreading of pathological tau protein. *Cellular and Molecular Life Sciences* **77**, 1721-1744, doi:10.1007/s00018-019-03349-1 (2020).

14 Colnaghi, L., Rondelli, D., Muzi-Falconi, M. & Sertic, S. Tau and DNA Damage in Neurodegeneration. *Brain Sci* **10**, 946, doi:10.3390/brainsci10120946 (2020).

15 Venkatramani, A. & Panda, D. Regulation of neuronal microtubule dynamics by tau: Implications for tauopathies. *International Journal of Biological*

Macromolecules **133**, 473-483, doi:https://doi.org/10.1016/j.ijbiomac.2019.04.120 (2019).
16 Brunello, C. A., Merezhko, M., Uronen, R.-L. & Huttunen, H. J. Mechanisms of secretion and spreading of pathological tau protein. *Cell Mol Life Sci* **77**, 1721-1744, doi:10.1007/s00018-019-03349-1 (2020).
17 Sallaberry, C. A. *et al.* Tau and Membranes: Interactions That Promote Folding and Condensation. *Front Cell Dev Biol* **9**, 725241-725241, doi:10.3389/fcell.2021.725241 (2021).
18 Zhang, H., Cao, Y., Ma, L., Wei, Y. & Li, H. Possible Mechanisms of Tau Spread and Toxicity in Alzheimer's Disease. *Front Cell Dev Biol* **9**, 707268, doi:10.3389/fcell.2021.707268 (2021).
19 Niewiadomska, G., Niewiadomski, W., Steczkowska, M. & Gasiorowska, A. Tau Oligomers Neurotoxicity. *Life* **11**, doi:10.3390/life11010028 (2021).
20 Ising, C. *et al.* NLRP3 inflammasome activation drives tau pathology. *Nature* **575**, 669-673, doi:10.1038/s41586-019-1769-z (2019).
21 Williamson, J. D. *et al.* Effect of Intensive vs Standard Blood Pressure Control on Probable Dementia: A Randomized Clinical Trial. *Jama* **321**, 553-561, doi:10.1001/jama.2018.21442 (2019).
22 Keren-Shaul, H. *et al.* A Unique Microglia Type Associated with Restricting Development of Alzheimer's Disease. *Cell* **169**, 1276-1290.e1217, doi:10.1016/j.cell.2017.05.018 (2017).
23 Kwon, H. S. & Koh, S.-H. Neuroinflammation in neurodegenerative disorders: the roles of microglia and astrocytes. *Translational Neurodegeneration* **9**, 42, doi:10.1186/s40035-020-00221-2 (2020).
24 Seol, Y. *et al.* How Microglia Manages Non-cell Autonomous Vicious Cycling of Aβ Toxicity in the Pathogenesis of AD. *Front Mol Neurosci* **13**, 593724-593724, doi:10.3389/fnmol.2020.593724 (2020).
25 Hansen, D. V., Hanson, J. E. & Sheng, M. Microglia in Alzheimer's disease. *Journal of Cell Biology* **217**, 459-472, doi:10.1083/jcb.201709069 (2017).
26 Lee, J.-H. *et al.* Astrocytes phagocytose adult hippocampal synapses for circuit homeostasis. *Nature* **590**, 612-617, doi:10.1038/s41586-020-03060-3 (2021).
27 Sanmarco, L. M., Polonio, C. M., Wheeler, M. A. & Quintana, F. J. Functional immune cell-astrocyte interactions. *J Exp Med* **218**, doi:10.1084/jem.20202715 (2021).
28 Bouvier, D. S. *et al.* The Multifaceted Neurotoxicity of Astrocytes in Ageing and Age-Related Neurodegenerative Diseases: A Translational Perspective. *Front Physiol* **13**, 814889, doi:10.3389/fphys.2022.814889 (2022).
29 Liddelow, S. A. *et al.* Neurotoxic reactive astrocytes are induced by activated microglia. *Nature* **541**, 481-487, doi:10.1038/nature21029 (2017).
30 Linnerbauer, M., Wheeler, M. A. & Quintana, F. J. Astrocyte Crosstalk in CNS Inflammation. *Neuron* **108**, 608-622, doi:https://doi.org/10.1016/j.neuron.2020.08.012 (2020).
31 Cantuti-Castelvetri, L. *et al.* Defective cholesterol clearance limits remyelination in the aged central nervous system. *Science* **359**, 684-688, doi:10.1126/science.aan4183 (2018).

32 Zhang, X., Huang, N., Xiao, L., Wang, F. & Li, T. Replenishing the Aged Brains: Targeting Oligodendrocytes and Myelination? *Front Aging Neurosci* **13**, 760200, doi:10.3389/fnagi.2021.760200 (2021).
33 Safaiyan, S. *et al.* Age-related myelin degradation burdens the clearance function of microglia during aging. *Nat Neurosci* **19**, 995-998, doi:10.1038/nn.4325 (2016).
34 Kaya, I. *et al.* Brain region-specific amyloid plaque-associated myelin lipid loss, APOE deposition and disruption of the myelin sheath in familial Alzheimer's disease mice. *J Neurochem* **154**, 84-98, doi:10.1111/jnc.14999 (2020).
35 Zhan, X. *et al.* Myelin basic protein associates with AβPP, Aβ1-42, and amyloid plaques in cortex of Alzheimer's disease brain. *J Alzheimers Dis* **44**, 1213-1229, doi:10.3233/jad-142013 (2015).
36 Thériault, P. & Rivest, S. Microglia: Senescence Impairs Clearance of Myelin Debris. *Current Biology* **26**, R772-R775, doi:https://doi.org/10.1016/j.cub.2016.06.066 (2016).
37 Nguyen, T. B. *et al.* DGAT1-Dependent Lipid Droplet Biogenesis Protects Mitochondrial Function during Starvation-Induced Autophagy. *Developmental Cell* **42**, 9-21.e25, doi:https://doi.org/10.1016/j.devcel.2017.06.003 (2017).
38 Ralhan, I., Chang, C. L., Lippincott-Schwartz, J. & Ioannou, M. S. Lipid droplets in the nervous system. *J Cell Biol* **220**, doi:10.1083/jcb.202102136 (2021).
39 Baker, D. J. & Petersen, R. C. Cellular senescence in brain aging and neurodegenerative diseases: evidence and perspectives. *J Clin Invest* **128**, 1208-1216, doi:10.1172/JCI95145 (2018).
40 Marschallinger, J. *et al.* Lipid-droplet-accumulating microglia represent a dysfunctional and proinflammatory state in the aging brain. *Nature Neuroscience* **23**, 194-208, doi:10.1038/s41593-019-0566-1 (2020).
41 Shimabukuro, M. K. *et al.* Lipid-laden cells differentially distributed in the aging brain are functionally active and correspond to distinct phenotypes. *Scientific Reports* **6**, 23795, doi:10.1038/srep23795 (2016).
42 Damulina, A. *et al.* White Matter Hyperintensities in Alzheimer's Disease: A Lesion Probability Mapping Study. *J Alzheimers Dis* **68**, 789-796, doi:10.3233/jad-180982 (2019).
43 Stone, D. B., Ryman, S. G., Hartman, A. P., Wertz, C. J. & Vakhtin, A. A. Specific White Matter Tracts and Diffusion Properties Predict Conversion From Mild Cognitive Impairment to Alzheimer's Disease. *Front Aging Neurosci* **13**, 711579, doi:10.3389/fnagi.2021.711579 (2021).
44 Kohama, S. G., Rosene, D. L. & Sherman, L. S. Age-related changes in human and non-human primate white matter: from myelination disturbances to cognitive decline. *Age (Dordr)* **34**, 1093-1110, doi:10.1007/s11357-011-9357-7 (2012).
45 Soldan, A. *et al.* White matter hyperintensities and CSF Alzheimer disease biomarkers in preclinical Alzheimer disease. *Neurology* **94**, e950-e960, doi:10.1212/WNL.0000000000008864 (2020).

46 Rizvi, B. *et al.* Association of Regional White Matter Hyperintensities With Longitudinal Alzheimer-Like Pattern of Neurodegeneration in Older Adults. *JAMA Netw Open* **4**, e2125166, doi:10.1001/jamanetworkopen.2021.25166 (2021).

47 Hays, C. C., Zlatar, Z. Z. & Wierenga, C. E. The Utility of Cerebral Blood Flow as a Biomarker of Preclinical Alzheimer's Disease. *Cell Mol Neurobiol* **36**, 167-179, doi:10.1007/s10571-015-0261-z (2016).

48 Duncombe, J. *et al.* Chronic cerebral hypoperfusion: a key mechanism leading to vascular cognitive impairment and dementia. Closing the translational gap between rodent models and human vascular cognitive impairment and dementia. *Clin Sci (Lond)* **131**, 2451-2468, doi:10.1042/cs20160727 (2017).

49 Miners, J. S. *et al.* Aβ degradation or cerebral perfusion? Divergent effects of multifunctional enzymes. *Frontiers in aging neuroscience* **6**, 238-238, doi:10.3389/fnagi.2014.00238 (2014).

50 Qiu, L. *et al.* Chronic cerebral hypoperfusion enhances Tau hyperphosphorylation and reduces autophagy in Alzheimer's disease mice. *Scientific Reports* **6**, 23964, doi:10.1038/srep23964 (2016).

51 ElAli, A., Thériault, P., Préfontaine, P. & Rivest, S. Mild chronic cerebral hypoperfusion induces neurovascular dysfunction, triggering peripheral beta-amyloid brain entry and aggregation. *Acta Neuropathologica Communications* **1**, 75, doi:10.1186/2051-5960-1-75 (2013).

52 Scheffer, S., Hermkens, D. M. A., van der Weerd, L., de Vries, H. E. & Daemen, M. J. A. P. Vascular Hypothesis of Alzheimer Disease. *Arteriosclerosis, Thrombosis, and Vascular Biology* **41**, 1265-1283, doi:10.1161/ATVBAHA.120.311911 (2021).

53 Escartin, C. *et al.* Reactive astrocyte nomenclature, definitions, and future directions. *Nat Neurosci* **24**, 312-325, doi:10.1038/s41593-020-00783-4 (2021).

54 Oakley, H. *et al.* Intraneuronal beta-amyloid aggregates, neurodegeneration, and neuron loss in transgenic mice with five familial Alzheimer's disease mutations: potential factors in amyloid plaque formation. *J Neurosci* **26**, 10129-10140, doi:10.1523/jneurosci.1202-06.2006 (2006).

55 Teitsdottir, U. D. *et al.* Association of glial and neuronal degeneration markers with Alzheimer's disease cerebrospinal fluid profile and cognitive functions. *Alzheimer's Research & Therapy* **12**, 92, doi:10.1186/s13195-020-00657-8 (2020).

56 Shipton, O. A., Tang, C. S., Paulsen, O. & Vargas-Caballero, M. Differential vulnerability of hippocampal CA3-CA1 synapses to Aβ. *Acta Neuropathologica Communications* **10**, 45, doi:10.1186/s40478-022-01350-7 (2022).

57 Youmans, K. L. *et al.* Intraneuronal Aβ detection in 5xFAD mice by a new Aβ-specific antibody. *Mol Neurodegener* **7**, 8, doi:10.1186/1750-1326-7-8 (2012).

58 Eimer, W. A. & Vassar, R. Neuron loss in the 5XFAD mouse model of Alzheimer's disease correlates with intraneuronal Aβ42 accumulation and

Caspase-3 activation. *Mol Neurodegener* **8**, 2, doi:10.1186/1750-1326-8-2 (2013).

59 Pichet Binette, A. *et al.* Bundle-specific associations between white matter microstructure and Aβ and tau pathology in preclinical Alzheimer's disease. *Elife* **10**, e62929, doi:10.7554/eLife.62929 (2021).

60 Collij, L. E. *et al.* White matter microstructure disruption in early stage amyloid pathology. *Alzheimer's & Dementia: Diagnosis, Assessment & Disease Monitoring* **13**, e12124, doi:https://doi.org/10.1002/dad2.12124 (2021).

61 Wang, Q. *et al.* Quantification of white matter cellularity and damage in preclinical and early symptomatic Alzheimer's disease. *NeuroImage: Clinical* **22**, 101767, doi:https://doi.org/10.1016/j.nicl.2019.101767 (2019).

62 Nasrabady, S. E., Rizvi, B., Goldman, J. E. & Brickman, A. M. White matter changes in Alzheimer's disease: a focus on myelin and oligodendrocytes. *Acta Neuropathologica Communications* **6**, 22, doi:10.1186/s40478-018-0515-3 (2018).

63 Montero-Crespo, M., Domínguez-Álvaro, M., Alonso-Nanclares, L., DeFelipe, J. & Blazquez-Llorca, L. Three-dimensional analysis of synaptic organization in the hippocampal CA1 field in Alzheimer's disease. *Brain* **144**, 553-573, doi:10.1093/brain/awaa406 (2021).

64 Medvedeva, Y. V., Ji, S. G., Yin, H. Z. & Weiss, J. H. Differential Vulnerability of CA1 versus CA3 Pyramidal Neurons After Ischemia: Possible Relationship to Sources of Zn²⁺ Accumulation and Its Entry into and Prolonged Effects on Mitochondria. *The Journal of Neuroscience* **37**, 726-737, doi:10.1523/jneurosci.3270-16.2016 (2017).

65 Perez-Cruz, C. *et al.* Reduced Spine Density in Specific Regions of CA1 Pyramidal Neurons in Two Transgenic Mouse Models of Alzheimer's Disease. *The Journal of Neuroscience* **31**, 3926, doi:10.1523/JNEUROSCI.6142-10.2011 (2011).

66 Di Paola, M. *et al.* Callosal atrophy in mild cognitive impairment and Alzheimer's disease: different effects in different stages. *Neuroimage* **49**, 141-149, doi:10.1016/j.neuroimage.2009.07.050 (2010).

67 Zhu, M. *et al.* Corpus callosum atrophy and cognitive decline in early Alzheimer's disease: longitudinal MRI study. *Dement Geriatr Cogn Disord* **37**, 214-222, doi:10.1159/000350410 (2014).

68 Kamphuis, W. *et al.* Glial fibrillary acidic protein isoform expression in plaque related astrogliosis in Alzheimer's disease. *Neurobiology of Aging* **35**, 492-510, doi:https://doi.org/10.1016/j.neurobiolaging.2013.09.035 (2014).

69 Escartin, C. *et al.* Reactive astrocyte nomenclature, definitions, and future directions. *Nature Neuroscience* **24**, 312-325, doi:10.1038/s41593-020-00783-4 (2021).

70 Braun, K., Antemano, R., Helmeke, C., Büchner, M. & Poeggel, G. Juvenile separation stress induces rapid region- and layer-specific changes in S100ß- and glial fibrillary acidic protein–immunoreactivity in astrocytes of the rodent medial prefrontal cortex. *Neuroscience* **160**, 629-638, doi:https://doi.org/10.1016/j.neuroscience.2009.02.074 (2009).

71 Cristóvão, J. S. & Gomes, C. M. S100 Proteins in Alzheimer's Disease. *Front Neurosci* **13**, 463-463, doi:10.3389/fnins.2019.00463 (2019).
72 Hovens, I., Nyakas, C. & Schoemaker, R. A novel method for evaluating microglial activation using ionized calcium-binding adaptor protein-1 staining: Cell body to cell size ratio. *Neuroimmunology and Neuroinflammation* **1**, 82-88, doi:10.4103/2347-8659.139719 (2014).
73 Michalovicz, L. T. *et al.* Astrocyte-specific transcriptome analysis using the ALDH1L1 bacTRAP mouse reveals novel biomarkers of astrogliosis in response to neurotoxicity. *Journal of Neurochemistry* **150**, 420-440, doi:https://doi.org/10.1111/jnc.14800 (2019).
74 Kenkhuis, B. *et al.* Iron loading is a prominent feature of activated microglia in Alzheimer's disease patients. *Acta Neuropathol Commun* **9**, 27, doi:10.1186/s40478-021-01126-5 (2021).
75 Ainscough, J. S. *et al.* Cathepsin S is the major activator of the psoriasis-associated proinflammatory cytokine IL-36γ. *Proc Natl Acad Sci U S A* **114**, E2748-e2757, doi:10.1073/pnas.1620954114 (2017).
76 Baranov, M. V. *et al.* The Phosphoinositide Kinase PIKfyve Promotes Cathepsin-S-Mediated Major Histocompatibility Complex Class II Antigen Presentation. *iScience* **11**, 160-177, doi:10.1016/j.isci.2018.12.015 (2019).
77 Ni, J. *et al.* The Critical Role of Proteolytic Relay through Cathepsins B and E in the Phenotypic Change of Microglia/Macrophage. *J Neurosci* **35**, 12488-12501, doi:10.1523/jneurosci.1599-15.2015 (2015).
78 Xie, Z. *et al.* Microglial cathepsin E plays a role in neuroinflammation and amyloid β production in Alzheimer's disease. *Aging Cell* **21**, e13565, doi:https://doi.org/10.1111/acel.13565 (2022).
79 Stadelmann, C., Timmler, S., Barrantes-Freer, A. & Simons, M. Myelin in the Central Nervous System: Structure, Function, and Pathology. *Physiological Reviews* **99**, 1381-1431, doi:10.1152/physrev.00031.2018 (2019).
80 Lloyd, A. F. & Miron, V. E. The pro-remyelination properties of microglia in the central nervous system. *Nature Reviews Neurology* **15**, 447-458, doi:10.1038/s41582-019-0184-2 (2019).
81 Couttas, T. A. *et al.* Loss of ceramide synthase 2 activity, necessary for myelin biosynthesis, precedes tau pathology in the cortical pathogenesis of Alzheimer's disease. *Neurobiology of Aging* **43**, 89-100, doi:https://doi.org/10.1016/j.neurobiolaging.2016.03.027 (2016).
82 Dean, D. C., III *et al.* Association of Amyloid Pathology With Myelin Alteration in Preclinical Alzheimer Disease. *JAMA Neurology* **74**, 41-49, doi:10.1001/jamaneurol.2016.3232 (2017).
83 Hoos, M. D., Ahmed, M., Smith, S. O. & Van Nostrand, W. E. Inhibition of familial cerebral amyloid angiopathy mutant amyloid beta-protein fibril assembly by myelin basic protein. *J Biol Chem* **282**, 9952-9961, doi:10.1074/jbc.M603494200 (2007).
84 Depp, C. *et al.* Ageing-associated myelin dysfunction drives amyloid deposition in mouse models of Alzheimer's disease. *bioRxiv*, 2021.2007.2031.454562, doi:10.1101/2021.07.31.454562 (2021).
85 Chen, J. F. *et al.* Enhancing myelin renewal reverses cognitive dysfunction

in a murine model of Alzheimer's disease. *Neuron* **109**, 2292-2307.e2295, doi:10.1016/j.neuron.2021.05.012 (2021).

86 Edmison, D., Wang, L. & Gowrishankar, S. Lysosome Function and Dysfunction in Hereditary Spastic Paraplegias. *Brain Sciences* **11**, 152 (2021).

87 Gowrishankar, S. *et al.* Massive accumulation of luminal protease-deficient axonal lysosomes at Alzheimer's disease amyloid plaques. *Proc Natl Acad Sci U S A* **112**, E3699-3708, doi:10.1073/pnas.1510329112 (2015).

88 Jack, C. R., Jr. *et al.* Age-specific and sex-specific prevalence of cerebral β-amyloidosis, tauopathy, and neurodegeneration in cognitively unimpaired individuals aged 50-95 years: a cross-sectional study. *Lancet Neurol* **16**, 435-444, doi:10.1016/s1474-4422(17)30077-7 (2017).

89 Livingston, G. *et al.* Dementia prevention, intervention, and care: 2020 report of the Lancet Commission. *Lancet* **396**, 413-446, doi:10.1016/s0140-6736(20)30367-6 (2020).